

UCLA
COMPUTATIONAL AND APPLIED MATHEMATICS

**A Maximum Principle Satisfying Modification of
Triangle Based Adaptive Stencils for the Solution
of Hyperbolic Conservation Laws**

Xu-Dong Liu

June 1991

CAM Report 91-11

Department of Mathematics
University of California, Los Angeles
Los Angeles, CA. 90024-1555

A Maximum Principle satisfying Modification of Triangle Based Adaptive Stencils for the Solution of Hyperbolic Conservation Laws

Xu-Dong Liu*

May 18, 1991

*Department of Mathematics, UCLA, Los Angeles, California, 90024. Research supported by NSF grant DM88-11863 and ONR grant N00014-86-k-0691.

Running head: Triangle Based Adaptive Stencils

Proofs sent to:

Xu-Dong Liu

Department of Mathematics, UCLA

Los Angeles, CA 90024

Subject classification: 65M05, 65M10

Keywords: Hyperbolic Conservation Laws, Limiters, Triangular Grid

Abstract

A modified triangle based adaptive difference stencil for the numerical approximation of hyperbolic conservation laws in two space dimensions is constructed. The scheme satisfies the maximum principle and approximates the flux with second order accuracy.

1 Introduction

In this article we modify a scheme developed by Louis J. Durlofsky, Bjorn Engquist and Stanley Osher [1]. Our modified scheme inherits all the advantages of the original scheme. For example, the modified scheme is a so-called second order accurate TVD scheme (i.e. formally second order accurate at the non-extrema of discrete solution and first order accurate at the extrema), which applies to an unstructured triangular grid. The scheme is based on a finite volume discretization and is particularly straightforward to implement. It relies on a very local adaptive interpolation idea, which results in computational efficiency. In addition to those virtues, the scheme satisfies the maximum principle in either the usual spatially independent flux case or variable coefficient flux with divergence free velocity field case. This is proven theoretically and numerically in this article. By a “maximum principle”, we mean both a maximum principle and minimum principle. The modified scheme costs only about 20% more computation than the original in our experiments. The scheme is almost the same as the original scheme except for some restrictions on triangulations, modifications in the limiting procedure , and in the variable coefficient flux case the divergence free velocity field is required in order to satisfy the maximum principle.

The outline of the article is as follows. In §2, we first discuss a condition for a solution of conservation law to satisfy the maximum principle. Then we describe finite volume space discretizations both in the spatially independent flux case and the variable coefficient flux case. Finally we present a TVD time discretization. In §3, we first present a triangulation, and, secondly, we then introduce concepts of real overshoot and undershoot, replacing the concepts of overshoot and undershoot in [1], we then select an appropriate linear interpolation from four candidates (the first three of them are exactly the same as described in [1]; however the last one is a constant). We then prove the scheme satisfies the maximum principle. Numerical experiments for constant and variable coefficient linear advection, as well as for nonlinear flux functions (Burgers’ equation and the Buckley-Levetett equation with source), are presented in §4.

2 Finite Volume Discretization

Before we present space and time discretizations, we observe that an obvious necessary condition for a solution of conservation law satisfying the maximum principle is the following: If a solution of conservation law

$$u_t + \vec{\nabla} \cdot \vec{F}(X, u, t) = 0$$

satisfies the maximum principle, then

$$\vec{\nabla}_X \cdot \vec{F}(X, u, t) = 0,$$

where X is a space vector.

In this article, we only consider two kinds of hyperbolic conservation laws. One has the usual spatially independent flux and the other has the variable coefficient flux with divergence free velocity field. We present them as following

$$\begin{aligned} u_t + \vec{\nabla} \cdot \vec{F} &= 0, \\ u(X, 0) &= u_o(X), \end{aligned} \quad (2.1)$$

where $\vec{F} = \vec{F}(u)$ in the former case and $\vec{F} = \vec{a}(X)f(u)$ in the latter case ($\vec{a}(X)$ is a velocity field satisfying $\vec{\nabla} \cdot \vec{a}(X) = 0$). Obviously the condition $\vec{\nabla}_X \cdot \vec{F}(X, u, t) = 0$ holds in both cases. That is the reason why the numerical solution of (2.1) has to satisfy the maximum principle.

As we mention in the abstract, we consider the hyperbolic conservation law (2.1) only in two space dimensions. We do the space discretization by the finite volume method using a triangular grid(See Fig 1). Integration of (2.1) over Δ_{ABC} gives

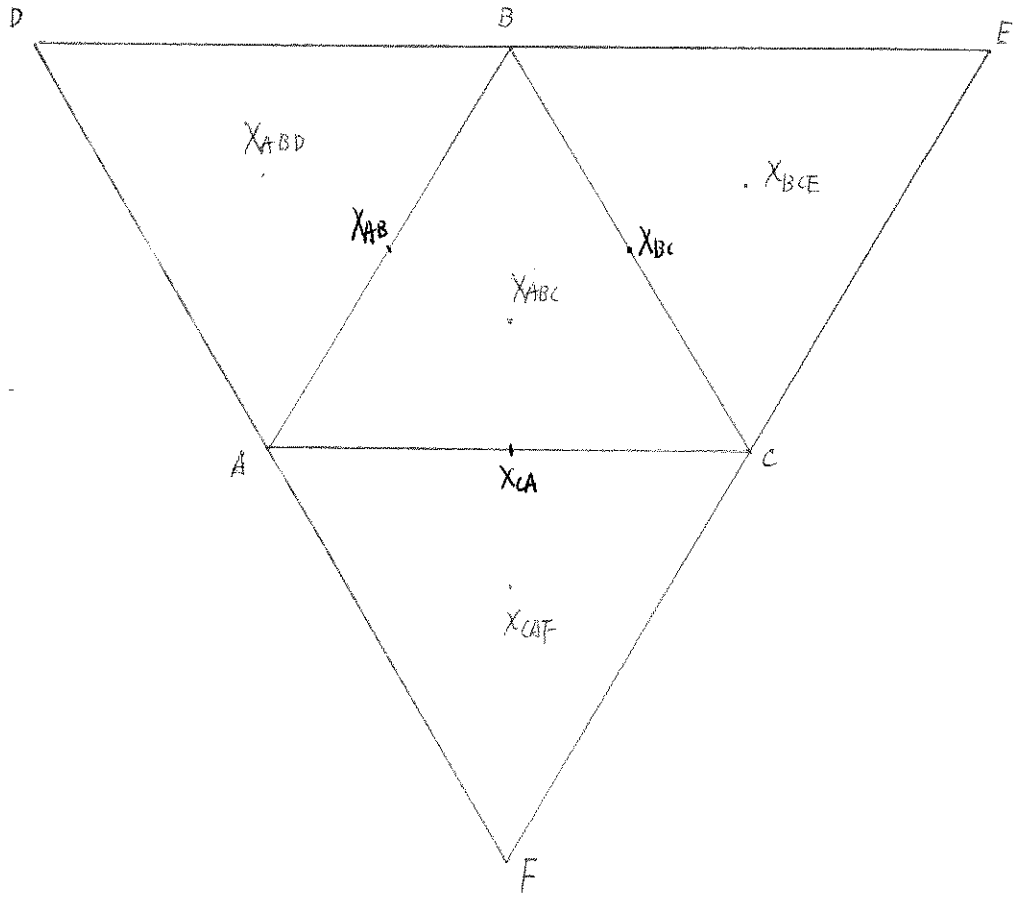
$$\frac{\partial}{\partial t} \int_{\Delta_{ABC}} u \, dA = - \int_{\Delta_{ABC}} (\vec{\nabla} \cdot \vec{F}) \, dA, \quad (2.2)$$

where Δ_{ABC} represents the region ABC . Applying the divergence theorem to the right hand side of (2.2) and defining

$$V_{ABC} = \int_{\Delta_{ABC}} u \, dA / |\Delta_{ABC}|$$

to be the average of u over Δ_{ABC} , where $|\Delta_{ABC}|$ denotes the area of Δ_{ABC} , gives us :

Fig 1



$$\frac{\partial}{\partial t} V_{ABC} = \frac{-1}{|\Delta_{ABC}|} [\int_{l_{AB}} \vec{F} \cdot \vec{n}_{AB} dl + \int_{l_{BC}} \vec{F} \cdot \vec{n}_{BC} dl + \int_{l_{CA}} \vec{F} \cdot \vec{n}_{CA} dl], \quad (2.3)$$

where \vec{n} is the outward unit normal. Obviously V_{ABC} is equal to the value of u evaluated at the triangle centroid X_{ABC} to within $O(|\Delta_{ABC}|)$.

To obtain second order accuracy, particularly in Δ_{ABC} , we construct a linear interpolation $L_{\Delta}(x)$ approximating the solution u in the triangular region Δ_{ABC} .

Let X_{AB} be the midpoint of the side AB , X_{BC} be the midpoint of the side BC , and X_{CA} be the midpoint of the side CA . Let $L_{\Delta}(X_{AB}^i)$ and $L_{\Delta}(X_{AB}^o)$ denote the limits of $L_{\Delta}(x)$ as $x \rightarrow X_{AB}$ from inside and outside triangle ABC respectively, and Let $L_{\Delta}(X_{BC}^i)$ and $L_{\Delta}(X_{BC}^o)$ denote the limits of $L_{\Delta}(x)$ as $x \rightarrow X_{BC}$ from inside and outside triangle ABC respectively, and Let $L_{\Delta}(X_{CA}^i)$ and $L_{\Delta}(X_{CA}^o)$ denote the limits of $L_{\Delta}(x)$ as $x \rightarrow X_{CA}$ from inside and outside triangle ABC respectively.

In the following several paragraphs in this section we are going to present the approximations to three line integrals $\int_{l_{AB}} \vec{F} \cdot \vec{n}_{AB} dl$, $\int_{l_{BC}} \vec{F} \cdot \vec{n}_{BC} dl$ and $\int_{l_{CA}} \vec{F} \cdot \vec{n}_{CA} dl$ in (2.3) to obtain our semi-discrete approximation to (2.3) in both the spatially independent flux case and the variable coefficient flux case.

We first consider the spatially independent flux case. At any side of Δ_{ABC} , say at AB , we introduce a two-point Lipschitz monotone flux $h_{AB}(\omega_1, \omega_2)$ which approximates $\vec{F} \cdot \vec{n}_{AB}$ in following sense

$$h_{AB}(\omega, \omega) = \vec{F}(\omega) \cdot \vec{n}_{AB},$$

where $h_{AB}(\omega_1, \omega_2)$ is a nondecreasing function of ω_1 , and a nonincreasing function of ω_2 , and has the conservation form

$$h_{AB}(\omega_1, \omega_2) = -h_{AB}(\omega_2, \omega_1).$$

The $h_{AB}(\omega_1, \omega_2)$ could be EO, Lax-Friedrichs, or Godunov flux (see [1] and references therein). Now by the midpoint formula for integral, our second order accurate, semi-discrete approximation to (2.3) is

$$L(V_{ABC}) \equiv \frac{\partial}{\partial t} V_{ABC}(t) = \frac{-1}{|\Delta_{ABC}|} [h_{AB}(L_{\Delta}(X_{AB}^i), L_{\Delta}(X_{AB}^o)) l_{AB} + h_{BC}(L_{\Delta}(X_{BC}^i), L_{\Delta}(X_{BC}^o)) l_{BC} + h_{CA}(L_{\Delta}(X_{CA}^i), L_{\Delta}(X_{CA}^o)) l_{CA}], \quad (2.4)$$

where l_{AB} is the length of the side AB , l_{BC} is the length of the side BC , and l_{CA} is the length of the side CA .

Now we consider the variable coefficient flux case. The line integrals

$$\begin{aligned}\int_{l_{AB}} \vec{F} \cdot \vec{n}_{AB} dl &= \int_{l_{AB}} \vec{n}_{AB} \cdot \vec{a}(X) f(u) dl, \\ \int_{l_{BC}} \vec{F} \cdot \vec{n}_{BC} dl &= \int_{l_{BC}} \vec{n}_{BC} \cdot \vec{a}(X) f(u) dl, \\ \int_{l_{CA}} \vec{F} \cdot \vec{n}_{CA} dl &= \int_{l_{CA}} \vec{n}_{CA} \cdot \vec{a}(X) f(u) dl.\end{aligned}$$

in (2.3). In order to approximate them, first we pick two of three sides of Δ_{ABC} arbitrarily, say AB and BC , and then we approximate the corresponding $\vec{n}_{AB} \cdot \vec{a}(X) f(u)$ and $\vec{n}_{BC} \cdot \vec{a}(X) f(u)$ also by two-point Lipschitz monotone flux functions $\vec{n}_{AB} \cdot \vec{a}(X) g(\omega_1, \omega_2)$ and $\vec{n}_{BC} \cdot \vec{a}(X) g(\omega_1, \omega_2)$ respectively, which approximate them in the following sense

$$\begin{aligned}\vec{n}_{AB} \cdot \vec{a}(X) g(\omega, \omega) &= \vec{n}_{AB} \cdot \vec{a}(X) f(\omega), \\ \vec{n}_{BC} \cdot \vec{a}(X) g(\omega, \omega) &= \vec{n}_{BC} \cdot \vec{a}(X) f(\omega),\end{aligned}$$

and they are nondecreasing functions of ω_1 and nonincreasing functions of ω_2 . By the midpoint formula for integral, we obtain

$$\begin{aligned}\int_{l_{AB}} \vec{F} \cdot \vec{n}_{AB} dl &= \vec{n}_{AB} \cdot \vec{a}(X_{AB}) l_{AB} g(L_{\Delta}(X_{AB}^i), L_{\Delta}(X_{AB}^o)), \\ \int_{l_{BC}} \vec{F} \cdot \vec{n}_{BC} dl &= \vec{n}_{BC} \cdot \vec{a}(X_{BC}) l_{BC} g(L_{\Delta}(X_{BC}^i), L_{\Delta}(X_{BC}^o)).\end{aligned}$$

Finally, at CA the last side of Δ_{ABC} , we approximate the line integral $\int_{l_{CA}} \vec{F} \cdot \vec{n}_{CA} dl$ by the following way

$$\int_{l_{CA}} \vec{F} \cdot \vec{n}_{CA} dl = \frac{(-\vec{n}_{AB} \cdot \vec{a}(X_{AB}) l_{AB} - \vec{n}_{BC} \cdot \vec{a}(X_{BC}) l_{BC})}{l_{CA}} l_{CA} g(L_{\Delta}(X_{CA}^i), L_{\Delta}(X_{CA}^o)).$$

It is easy to understand that $\frac{(-\vec{n}_{AB} \cdot \vec{a}(X_{AB}) l_{AB} - \vec{n}_{BC} \cdot \vec{a}(X_{BC}) l_{BC})}{l_{CA}} g(\omega_1, \omega_2)$ is also two-point Lipschitz monotone flux function, which is nondecreasing function of ω_1 and nonincreasing function of ω_2 . We denote

$$\begin{aligned}h_{AB}(L_{\Delta}(X_{AB}^i), L_{\Delta}(X_{AB}^o)) &= \vec{n}_{AB} \cdot \vec{a}(X_{AB}) g(L_{\Delta}(X_{AB}^i), L_{\Delta}(X_{AB}^o)), \\ h_{BC}(L_{\Delta}(X_{BC}^i), L_{\Delta}(X_{BC}^o)) &= \vec{n}_{BC} \cdot \vec{a}(X_{BC}) g(L_{\Delta}(X_{BC}^i), L_{\Delta}(X_{BC}^o)), \\ h_{CA}(L_{\Delta}(X_{CA}^i), L_{\Delta}(X_{CA}^o)) &= \frac{(-\vec{n}_{AB} \cdot \vec{a}(X_{AB}) l_{AB} - \vec{n}_{BC} \cdot \vec{a}(X_{BC}) l_{BC})}{l_{CA}} \\ &\quad \cdot g(L_{\Delta}(X_{CA}^i), L_{\Delta}(X_{CA}^o)).\end{aligned}$$

We obtain our second order accurate, semi-discrete approximation (2.4) in the variable coefficient flux case.

Remark : There are three things we have to mention here.

The first is that in both cases the approximation (2.4) is weakly second order accurate in the sense that each of three flux terms is within $O(l^2)$ of the line integrals, $\int_l \vec{F} \cdot \vec{n} dl/l$, along the corresponding interfaces.

The second is that in the spatially independent flux case, by the divergence theorem, the following formula :

$$h_{AB}(c, c)l_{AB} + h_{BC}(c, c)l_{BC} + h_{CA}(c, c)l_{CA} = 0, \quad c = \text{constant}, \quad (2.5)$$

holds. Also in the variable coefficient case, the way we shall approximate the line integrals, the formula (2.5) will also hold. Actually we made the velocity field numerically divergence free according to the nature of the divergence free velocity field. The formula (2.5) is critical to prove that our scheme satisfies the maximum principle in §3.

The last is that the approximation (2.4) has the conservation form that the $h_{AB}(L_\Delta(X_{AB}^i), L_\Delta(X_{AB}^o))$ is equal to the $-h_{AB}(L_\Delta(X_{AB}^o), L_\Delta(X_{AB}^i))$ in the spatially independent flux case, and the $h_{AB}(L_\Delta(X_{AB}^i), L_\Delta(X_{AB}^o))$ is equal to the $-h_{AB}(L_\Delta(X_{AB}^o), L_\Delta(X_{AB}^i))$ within $O(l^3)$ or the total numerical flux through the boundaries is equal to the total flux through the boundaries within $O(l^1)$ in the variable coefficient flux case.

Now the right hand side of (2.4) can be evaluated and $V_{ABC}(t)$ can be integrated in time. The time integration is accomplished via a second order TVD Runge-Kutta procedure (see [2]) :

$$\begin{aligned} V_{ABC}^1 &= V_{ABC} + \Delta t L(V_{ABC}) \\ V_{ABC}^{new} &= \frac{1}{2}V_{ABC} + \frac{1}{2}(V_{ABC}^1 + \Delta t L(V_{ABC}^1)), \end{aligned}$$

where $V_{ABC} = V_{ABC}(t_n)$, $V_{ABC}(t_{n+1}) = V_{ABC}^{new}$.

3 The Construction of Our Scheme

3.1 Triangulation

When we do a triangulation, we have to keep in mind the possibility of strange boundary shapes, e.g. wedges. We also prefer regular triangulations because regular ones can avoid overshoot or undershoot that is not caused by

the approximated solution itself. The triangulations we are going to introduce are rather regular, but they also can deal with wedge shaped boundaries (see Fig 2).

The triangulation should satisfy the following restrictions :

(i) The midpoints X_{CA} and X_{BC} are in the triangular region of

$$\Delta_{X_{AB}X_{BCE}X_{CAF}};$$

(ii) The midpoints X_{BC} and X_{AB} are in the triangular region of

$$\Delta_{X_{CA}X_{BCE}X_{ABD}};$$

(iii) The midpoints X_{AB} and X_{CA} are in the triangular region of

$$\Delta_{X_{BC}X_{ABD}X_{CAF}}.$$

These three restrictions have to be satisfied at the same time.

3.2 Linear Interpolation

3.2.1 Notation

Definition (3.1)

Call X_i a nearby point of X_{ABC} , if it belongs to a triangle element that has at least a common point with the triangle element Δ_{ABC} . We denote the set of all the nearby points of X_{ABC} by $N(X_{ABC})$.

Definition (3.2)

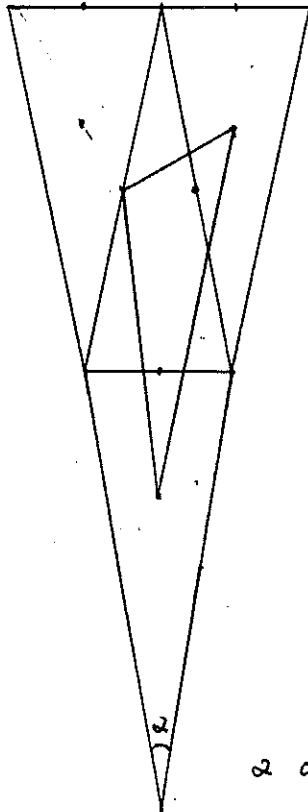
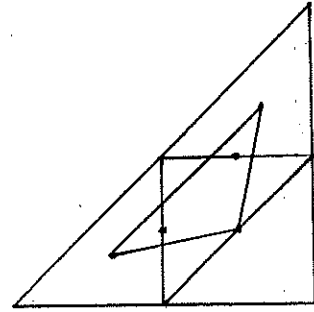
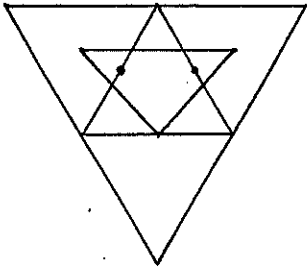
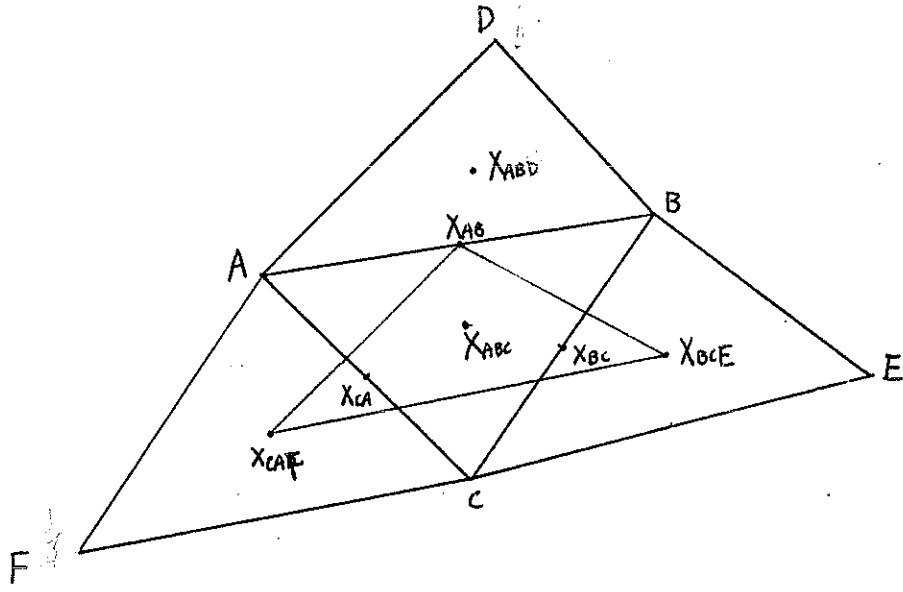
Local Upper Bound of the element Δ_{ABC} :

$$UB_{ABC} = \max(V_k) \\ X_k \in N(X_{ABC})$$

Local Lower Bound of the element Δ_{ABC} :

$$LB_{ABC} = \min(V_k) \\ X_k \in N(X_{ABC})$$

Fig 2



11

α could be very small

3.2.2 Construction of the Linear Interpolation L_Δ

There are three candidates for L_Δ , noted as L_Δ^1 , L_Δ^2 , and L_Δ^3 . L_Δ^1 is the linear interpolatant of the three pairs of point and corresponding value

$$(X_{ABC}, V_{ABC}), (X_{BCE}, V_{BCE}), (X_{CAF}, V_{CAF}),$$

L_Δ^2 is the linear interpolatant of the three pairs of point and corresponding value

$$(X_{ABC}, V_{ABC}), (X_{CAF}, V_{CAF}), (X_{ABD}, V_{ABD}),$$

and L_Δ^3 is the linear interpolatant of the three pairs of point and corresponding value

$$(X_{ABC}, V_{ABC}), (X_{ABD}, V_{ABD}), (X_{BCE}, V_{BCE})$$

(see Fig 3). Here and below we assume that the three triangle centroids i.e. X_{ABC} , X_{BCE} and X_{CAF} are not collinear. At this point, three L_Δ^i ($i = 1, 2, 3$) are possible, and a limited version of L_Δ can be selected from them.

Before we describe to the selection of a proper L_Δ^i , we introduce the concepts of real overshoot and undershoot.

Definition (3.3)

If for any L_Δ^i ($i = 1, 2, 3$), one of the following two inequalities is violated

$$\begin{aligned} UB_{ABC} &\geq \max(L_\Delta^i(X_{AB}), L_\Delta^i(X_{BC}), L_\Delta^i(X_{CA})) \\ LB_{ABC} &\leq \min(L_\Delta^i(X_{AB}), L_\Delta^i(X_{BC}), L_\Delta^i(X_{CA})), \end{aligned} \quad (3.1)$$

we say that **real overshoot** (if the first one is violated) or **real undershoot** (if the second one is violated) occurs at element Δ_{ABC} .

3.2.3 The Selection of L_Δ

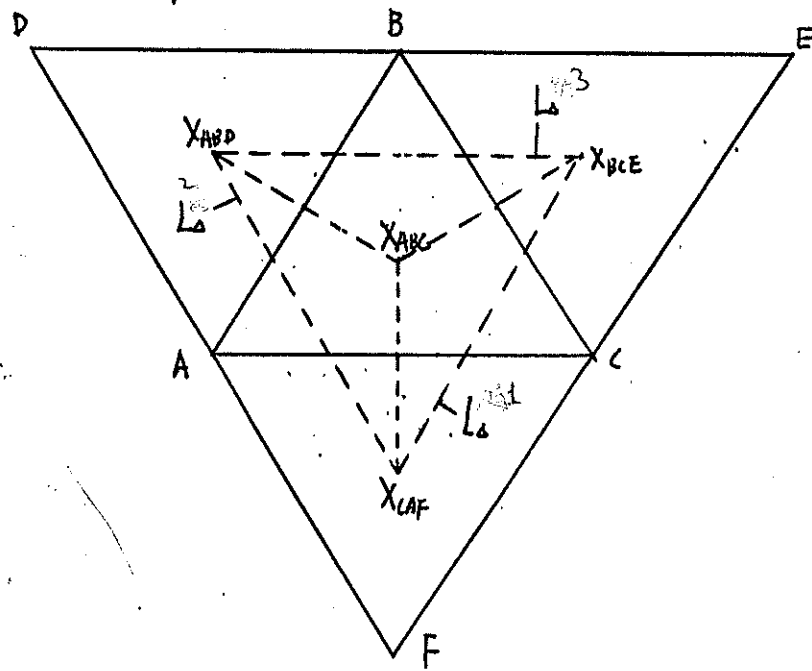
Following and modifying the selection procedure in [1], we select the L_Δ^i for which $|\nabla L_\Delta^i|$ is maximized, and no real overshoot and undershoot occurs.

The procedure is as follows :

(i) We first compute the magnitude of the gradient of each L_Δ^i

$$|\nabla L_\Delta^i| \equiv [(\frac{\partial}{\partial x} L_\Delta^i)^2 + \frac{\partial}{\partial y} L_\Delta^i]^{\frac{1}{2}} \quad i = 1, 2, 3$$

Fig 3



(ii) From the L_{Δ}^i for which $|\nabla L_{\Delta}^i|$ is the maximum, through the L_{Δ}^i for which $|\nabla L_{\Delta}^i|$ is the second largest, to the L_{Δ}^i for which $|\nabla L_{\Delta}^i|$ is the minimum, we check if

$$L_{\Delta}^i(X_i) \text{ is between } V_{ABC} \text{ and } \begin{array}{ll} V_{ABD} & \text{if } i = 1 \\ V_{BCE} & \text{if } i = 2 \\ V_{CAF} & \text{if } i = 3 \end{array}$$

is satisfied, where $X_1 = X_{AB}$, $X_2 = X_{BC}$ and $X_3 = X_{CA}$. If L_{Δ}^i is the first one satisfying this requirement, then L_{Δ}^i is chosen to be the appropriate L_{Δ} (and from the triangulation we have (3.1) holds). If no L_{Δ}^i satisfies this requirement, which means overshoot or undershoot, we go to (iii).

(iii) We compute the Local Upper Bound UB_{ABC} and the Local Lower Bound LB_{ABC} .

(iv) From the L_{Δ}^i for which $|\nabla L_{\Delta}^i|$ is the maximum, through the L_{Δ}^i for which $|\nabla L_{\Delta}^i|$ is the second largest, to the L_{Δ}^i for which $|\nabla L_{\Delta}^i|$ is the minimum, we check if (3.1) .i.e

$$\begin{aligned} UB_{ABC} &\geq \max(L_{\Delta}^i(X_{AB}), L_{\Delta}^i(X_{BC}), L_{\Delta}^i(X_{CA})) \\ LB_{ABC} &\leq \min(L_{\Delta}^i(X_{AB}), L_{\Delta}^i(X_{BC}), L_{\Delta}^i(X_{CA})) \end{aligned}$$

is satisfied. If L_{Δ}^i is the first one satisfying both inequalities, then L_{Δ}^i is chosen to be appropriate L_{Δ} . If no L_{Δ}^i satisfies both inequalities, then we choose

$$L_{\Delta} \equiv V_{ABC}.$$

In the last case the accuracy reduces from second order to first order. However, (3.1) holds in all cases.

3.3 Maximum Principle

Theorem For the hyperbolic conservation law (2.1), our scheme (with the triangulation, the linear interpolation, and the 2nd order TVD Runge-Kutta time discretization) satisfies the maximum principle under the CFL condition :

$$\Delta t \sigma (\sup | \frac{d\vec{F}}{du} |) \leq \frac{1}{3},$$

where $\sigma = \sup(L_{\Delta_{ABC}} / | \Delta_{ABC} |)$, which is evaluated over all the triangles in the grid. $L_{\Delta_{ABC}}$ and $| \Delta_{ABC} |$ denote the perimeter and area of Δ_{ABC} , respectively.

Proof:

For any Δ_{ABC}

$$L(V_{ABC}) \equiv \frac{\partial}{\partial t} V_{ABC}(t) = \frac{-1}{|\Delta_{ABC}|} [h_{AB}(L_{\Delta}(X_{AB}^i), L_{\Delta}(X_{AB}^o))l_{AB} \\ + h_{BC}(L_{\Delta}(X_{BC}^i), L_{\Delta}(X_{BC}^o))l_{BC} \\ + h_{CA}(L_{\Delta}(X_{CA}^i), L_{\Delta}(X_{CA}^o))l_{CA}].$$

Denote

$$\bar{U}B_{ABC} \equiv \max(V_i, \\ X_i \in N(X_j) \\ X_j \in N(X_{ABC}))$$

and $V'_{ABC} = \min(L_{\Delta}(X_{AB}^i), L_{\Delta}(X_{BC}^i), L_{\Delta}(X_{CA}^i))$. Due to the triangulation and linear interpolate, (3.1) holds. we have

$$\bar{U}B_{ABC} \geq \max(L_{\Delta}(X_{AB}^o), L_{\Delta}(X_{BC}^o), L_{\Delta}(X_{CA}^o)).$$

From the monotonic property of the flux, we obtain

$$L(V_{ABC}) \leq \frac{-1}{|\Delta_{ABC}|} [h_{AB}(V'_{ABC}, \bar{U}B_{ABC})l_{AB} + \\ h_{BC}(V'_{ABC}, \bar{U}B_{ABC})l_{BC} + \\ h_{CA}(V'_{ABC}, \bar{U}B_{ABC})l_{CA}]. \quad (3.2)$$

From the formula (2.5),

$$0 = h_{AB}(V'_{ABC}, V'_{ABC})l_{AB} + h_{BC}(V'_{ABC}, V'_{ABC})l_{BC} \\ + h_{CA}(V'_{ABC}, V'_{ABC})l_{CA} \quad (3.3)$$

holds. Add (3.2) and (3.3), we get

$$L(V_{ABC}) \leq \frac{-1}{|\Delta_{ABC}|} [h_{AB}(V'_{ABC}, \bar{U}B_{ABC})l_{AB} - h_{AB}(V'_{ABC}, V'_{ABC})l_{AB} + \\ h_{BC}(V'_{ABC}, \bar{U}B_{ABC})l_{BC} - h_{BC}(V'_{ABC}, V'_{ABC})l_{BC} + \\ h_{CA}(V'_{ABC}, \bar{U}B_{ABC})l_{CA} - h_{CA}(V'_{ABC}, V'_{ABC})l_{CA}] \\ = \frac{-1}{|\Delta_{ABC}|} [(h_{AB}(V'_{ABC}, \xi_1))'(\bar{U}B_{ABC} - V'_{ABC})l_{AB} + \\ (h_{BC}(V'_{ABC}, \xi_2))'(\bar{U}B_{ABC} - V'_{ABC})l_{BC} + \\ (h_{CA}(V'_{ABC}, \xi_3))'(\bar{U}B_{ABC} - V'_{ABC})l_{CA}];$$

Hence,

$$L(V_{ABC}) \leq \frac{1}{|\Delta_{ABC}|} [\sup \left| \frac{dF}{du} \right| (\bar{U}B_{ABC} - V'_{ABC})(l_{AB} + l_{BC} + l_{CA})].$$

Thus,

$$L(V_{ABC}) \leq \frac{L_{\Delta ABC}}{|\Delta_{ABC}|} \sup \left| \frac{dF}{du} \right| (\bar{U}B_{ABC} - V'_{ABC}),$$

where $L_{\Delta ABC} = l_{AB} + l_{BC} + l_{CA}$.

By the same analysis we obtain

$$L(V_{ABC}) \geq \frac{L_{\Delta ABC}}{|\Delta_{ABC}|} \sup \left| \frac{dF}{du} \right| (\bar{L}B_{ABC} - V''_{ABC}),$$

where $V''_{ABC} = \max(L_{\Delta}(X_{AB}^i), L_{\Delta}(X_{BC}^i), L_{\Delta}(X_{CA}^i))$ and

$$\begin{aligned} \bar{L}B_{ABC} &\equiv \min(V_i) \\ &X_i \in N(X_j) \\ &X_j \in N(X_{ABC}). \end{aligned}$$

Now we perform the time discretization. First we try the Euler forward time discretization and obtain

$$V_{ABC}^1 = V_{ABC} + \Delta t L(V_{ABC}),$$

or

$$\begin{aligned} V_{ABC}^1 &\leq V_{ABC} + \Delta t \frac{L_{\Delta ABC}}{|\Delta_{ABC}|} \sup \left| \frac{dF}{du} \right| (\bar{U}B_{ABC} - V'_{ABC}) \\ &\leq V_{ABC} + \Delta t \sigma \sup \left| \frac{dF}{du} \right| (\bar{U}B_{ABC} - V'_{ABC}). \end{aligned}$$

From the CFL condition,

$$V_{ABC}^1 \leq V_{ABC} + \frac{1}{3}(\bar{U}B_{ABC} - V'_{ABC}).$$

From a lemma which will be proven below,

$$\frac{1}{3}(\bar{U}B_{ABC} - V'_{ABC}) \leq \bar{U}B_{ABC} - V_{ABC}$$

holds. Hence,

$$\begin{aligned} V_{ABC}^1 &\leq V_{ABC} + (\bar{U}B_{ABC} - V_{ABC}) \\ &= \bar{U}B_{ABC}. \end{aligned}$$

By the same analysis, we get

$$\bar{L}B_{ABC} \leq V_{ABC}^1 \leq \bar{U}B_{ABC},$$

or

$$\begin{aligned} \min(V_i) &\leq V_{ABC}^1 \leq \max(V_i) \\ X_i \in N(X_j) & \quad X_i \in N(X_j) \\ X_j \in N(X_{ABC}) & \quad X_j \in N(X_{ABC}). \end{aligned}$$

Hence V_{ABC}^1 is bounded by the values V at nearby points of nearby point of X_{ABC} , or we can say for the Euler forward time discretization that the scheme satisfies the maximum principle.

Now we consider the 2nd order TVD Runge-Kutta time discretization :

$$\begin{aligned} V_{ABC}^1 &= V_{ABC} + \Delta t L(V_{ABC}) \\ V_{ABC}^{new} &= \frac{1}{2}V_{ABC} + \frac{1}{2}(V_{ABC}^1 + \Delta t L(V_{ABC}^1)) \end{aligned}$$

(see paper [2]).

Since the 2nd order TVD Runge-Kutta is substantially a combination of two one-step Euler forward, the maximum principle is also satisfied by the former one.

The proof will follow if we prove the following lemma.

Lemma

If

$$\begin{aligned} V'_{ABC} &= \min(L_{\Delta}(X_{AB}^i), L_{\Delta}(X_{BC}^i), L_{\Delta}(X_{CA}^i)) \\ V''_{ABC} &= \max(L_{\Delta}(X_{AB}^i), L_{\Delta}(X_{BC}^i), L_{\Delta}(X_{CA}^i)) \\ V_{ABC} &= \frac{1}{3}(L_{\Delta}(X_{AB}^i) + L_{\Delta}(X_{BC}^i) + L_{\Delta}(X_{CA}^i)), \end{aligned}$$

Then

$$\begin{aligned} \frac{1}{3}(\bar{U}B_{ABC} - V'_{ABC}) &\leq \bar{U}B_{ABC} - V_{ABC} \\ \frac{1}{3}(\bar{L}B_{ABC} - V''_{ABC}) &\geq \bar{L}B_{ABC} - V_{ABC}. \end{aligned}$$

Proof:

$$\begin{aligned} &\bar{U}B_{ABC} - V'_{ABC} \\ &= \bar{U}B_{ABC} - \frac{1}{3}(L_{\Delta}(X_{AB}^i) + L_{\Delta}(X_{BC}^i) + L_{\Delta}(X_{CA}^i)) \\ &\quad + \frac{1}{3}(L_{\Delta}(X_{AB}^i) - V'_{ABC} + L_{\Delta}(X_{BC}^i) - V'_{ABC} + L_{\Delta}(X_{CA}^i) - V'_{ABC}) \\ &= \bar{U}B_{ABC} - V_{ABC} \\ &\quad + \frac{1}{3}(L_{\Delta}(X_{AB}^i) - V'_{ABC} + L_{\Delta}(X_{BC}^i) - V'_{ABC} + L_{\Delta}(X_{CA}^i) - V'_{ABC}) \\ &\leq \bar{U}B_{ABC} - V_{ABC} + \frac{2}{3}(\bar{U}B_{ABC} - V'_{ABC}). \end{aligned}$$

Hence,

$$\frac{1}{3}(\bar{U}B_{ABC} - V'_{ABC}) \leq \bar{U}B_{ABC} - V_{ABC}.$$

By the same analysis,

$$\frac{1}{3}(\bar{L}B_{ABC} - V''_{ABC}) \geq \bar{L}B_{ABC} - V_{ABC}$$

also holds.

At the end of this section, we contrast our scheme with the scheme introduced by Cockburn, Hou, and Shu in [3]. Their scheme is formally uniformly 2-nd order accurate if one is able to choose a proper parameter M , and ours is 2-nd order accurate in the sense of flux approximation always. Their scheme satisfies the maximum principle within $O(h)$ globally, which means the violation is negligible, and ours strictly satisfies the maximum principle. Their scheme is less restrictive on triangulation than ours, but their CFL condition ($CFL = \frac{1}{3\delta(1+4\mu b)}$ where b is the upper bound of boundary function and initial function) is more restrictive than ours ($CFL = \frac{1}{3}$). Their scheme satisfies the maximum principle more locally (the approximating solution is bounded by previous values at four nearby points) than ours (ours involves more nearby points). However, ours is parameter free.

4 The Numerical Experiments

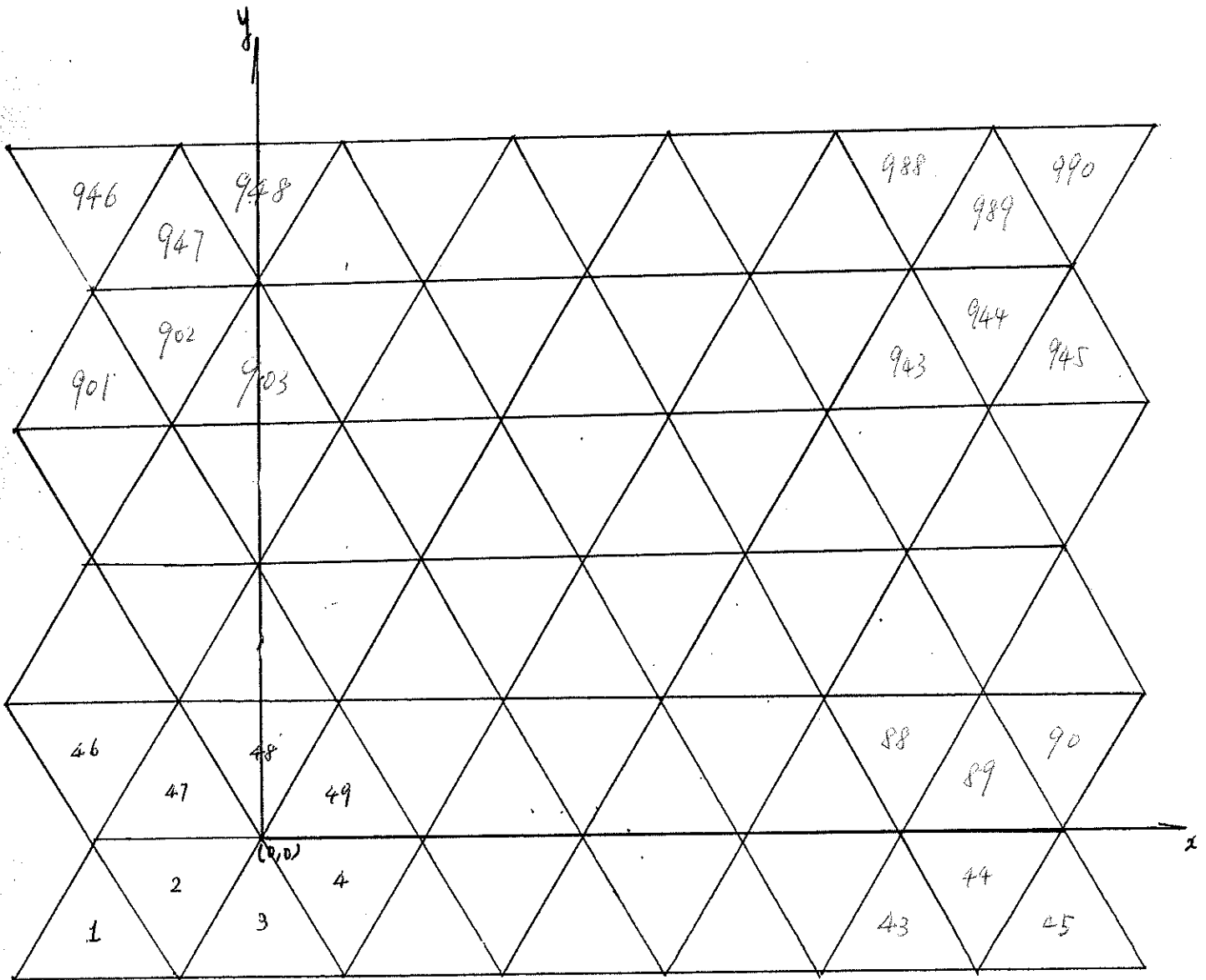
In this section we present some numerical experiments for conservation law. In all of our experiments, the solution region is a rectangle domain discretized via an equilateral triangulation with 990 elements, as shown in Fig 4 (a integer number in a triangle is the indicator of the triangle and V_n is the value of the numerical solution at the centroid of the n -th triangle). Periodic boundary conditions are imposed in both the x - and the y - directions; the initial condition is similarly x - and y - periodic, unless otherwise noted. The numerical results are plotted by contour plots.

First, we give an experiment which shows the original scheme violates the maximum principle.

For conservation law $u_t - \frac{\sqrt{3}}{2}u_x + \frac{1}{2}u_y = 0$ or $u_t + \nabla \cdot (\vec{a}u) = 0$, where the velocity field $\vec{a} = (-\frac{\sqrt{3}}{2}, \frac{1}{2})^T$, the original scheme with a upwind flux is

$$\frac{\partial}{\partial t} V_{ABC} = \frac{-1}{|\Delta_{ABC}|} [\begin{aligned} & \max(\vec{a} \cdot \vec{n}_{AB}, 0) L_{\Delta}(X_{AB}^i) l_{AB} + \\ & \min(\vec{a} \cdot \vec{n}_{AB}, 0) L_{\Delta}(X_{AB}^o) l_{AB} + \\ & \max(\vec{a} \cdot \vec{n}_{BC}, 0) L_{\Delta}(X_{BC}^i) l_{BC} + \\ & \min(\vec{a} \cdot \vec{n}_{BC}, 0) L_{\Delta}(X_{BC}^o) l_{BC} + \\ & \max(\vec{a} \cdot \vec{n}_{CA}, 0) L_{\Delta}(X_{CA}^i) l_{CA} + \\ & \min(\vec{a} \cdot \vec{n}_{CA}, 0) L_{\Delta}(X_{CA}^o) l_{CA}]. \end{aligned}$$

Fig 4



For an equilateral triangulation (the simplest triangulation, see Fig 5), at the element Δ_{ABC} , we have $\vec{a} \cdot \vec{n}_{AB} = 0$, $\vec{a} \cdot \vec{n}_{BC} = -\frac{\sqrt{3}}{2}$, $\vec{a} \cdot \vec{n}_{CA} = \frac{\sqrt{3}}{2}$. Thus,

$$\frac{\partial}{\partial t} V_{ABC} = \frac{-1}{|\Delta_{ABC}|} \left[-\frac{\sqrt{3}}{2} L_{\Delta}(X_{BC}^o) + \frac{\sqrt{3}}{2} L_{\Delta}(X_{CA}^i) \right] l,$$

where $l = l_{AB} = l_{BC} = l_{CA}$. For special data $V : V_{ACJ} = \frac{1}{2}$, $V_{ABD} = V_{ADF} = V_{BDH} = 0$, the others are 1, by the original scheme, $L_{\Delta}(X_{BC}^o) = 1$ and $L_{\Delta}(X_{CA}^i) = \frac{3}{4}$. Hence,

$$\frac{\partial}{\partial t} V_{ABC} = \frac{-l}{|\Delta_{ABC}|} \left[-\frac{\sqrt{3}}{2} \cdot 1 + \frac{\sqrt{3}}{2} \cdot \frac{3}{4} \right] = \frac{\sqrt{3}}{8} \frac{l}{|\Delta_{ABC}|} > 0.$$

Note that $V_{ABC} = 1.0$ is the maximum. Hence, the original scheme violates the maximum principle.

For any linear conservation law $u_t + \nabla \cdot (\vec{a}(x)u) = 0$, by a upwind flux, we have

$$h(\omega_1, \omega_2) = \max((\vec{a}(x) \cdot \vec{n}), 0)\omega_1 + \min((\vec{a}(x) \cdot \vec{n}), 0)\omega_2.$$

For a linear conservation law $u_t + (-1) \cdot u_x + (0) \cdot u_y = 0$ with special initial data ($V_{471} = 0.5$, $V_{516} = V_{517} = V_{518} = 0.0$ and the others are 1.0) which are substantially the same data in the previous experiment, the numerical results show that the original scheme violates the maximum principle (at $t = 0.24$, $\max(V_n) = 1.063 > 1.0$ and $\min(V_n) = 0.2578$, and also see Fig 6) and the modified scheme does not (at $t = 0.24$, $\max(V_n) = 1.0$ and $\min(V_n) = 0.3333 > 0.0$, and also see Fig 7).

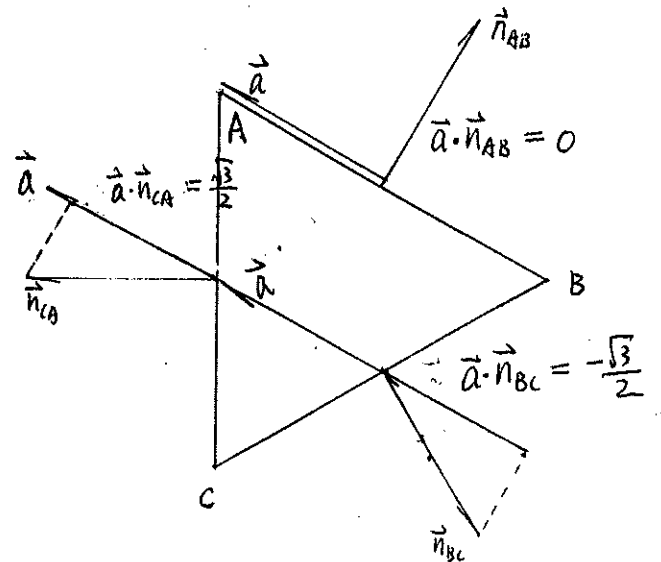
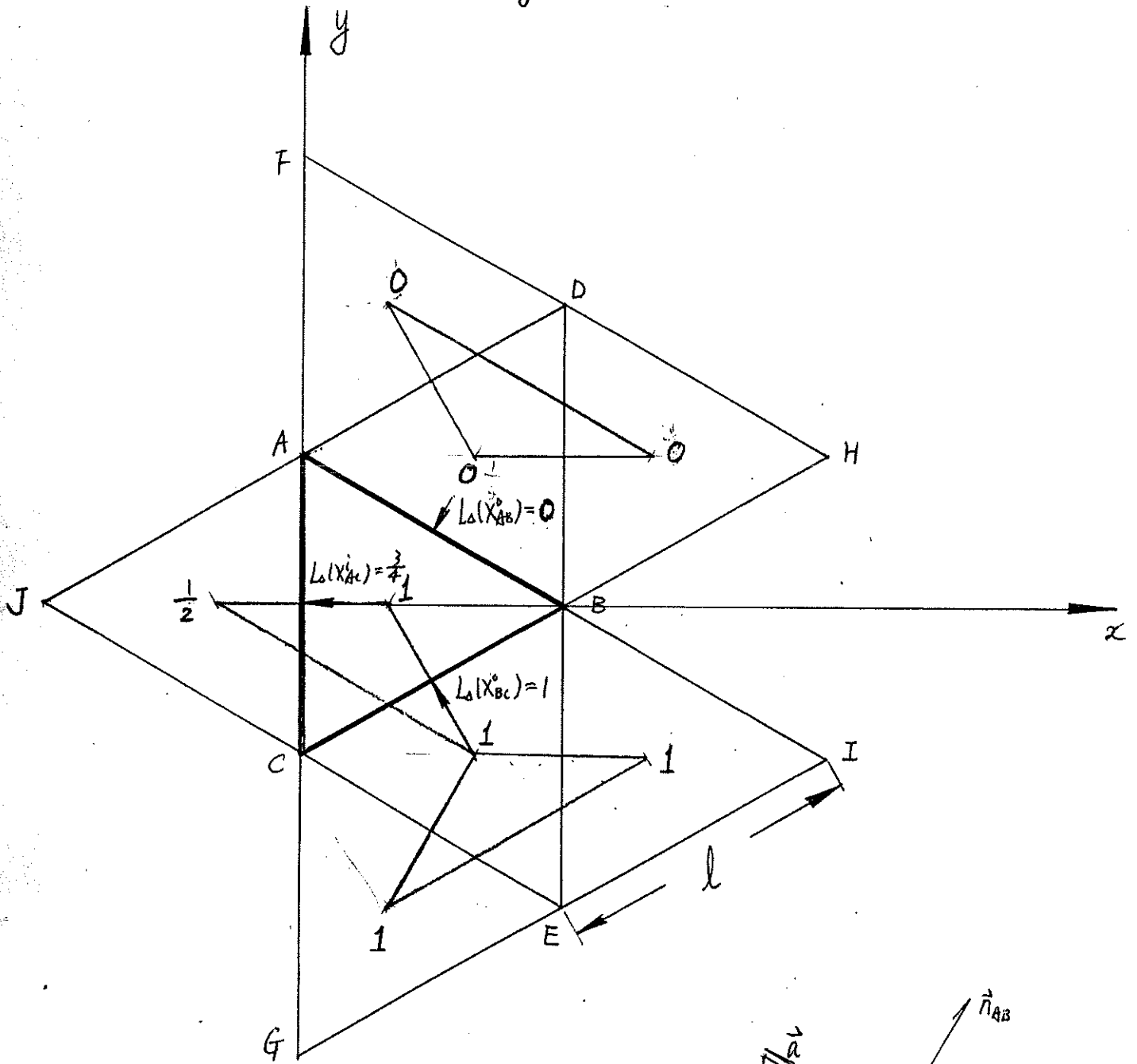
We next consider the same linear conservation law with initial data $u_o(x, y) = \sin(2\pi x)\sin(\frac{4\pi y}{\sqrt{3}})$ (see Fig 8). The numerical result show that the modified scheme satisfies the maximum principle (at $t = 0.72$, $\max(V_n) = 0.9126 < 1.0$ and $\min(V_n) = -0.8519 > -1.0$, and also see Fig 9).

For Burgers' equation $u_t + \nabla \cdot (\frac{1}{2}u^2\vec{a}) = 0$, by the *EO* flux, we obtain

$$h(\omega_1, \omega_2) = \omega_1 \max\left(\left(\frac{n_1+n_2}{2}\right)\omega_1, 0\right) + \omega_2 \min\left(\left(\frac{n_1+n_2}{2}\right)\omega_2, 0\right),$$

where n_1 and n_2 represent the components of \vec{n} . With initial data $u_o(x, y) = \sin(2\pi x)\sin(\frac{4\pi y}{\sqrt{3}})$ (see Fig 8), the numerical results show again that the original scheme violates the maximum principle (at $t = 0.24$, $\max(V_n) = 1.12 > 1.0$ and $\min(V_n) = -1.15 < -1.0$, and also see Fig 10) and the modified scheme does not (at $t = 0.24$, $\max(V_n) = 0.9113 < 1.0$ and $\min(V_n) =$

Fig 95



$-0.9025 > -1.0$, and also see Fig 11, and at $t = 1.0$, $\max(V_n) = 0.6000 < 1.0$ and $\min(V_n) = -0.5891 > -1.0$, and also see Fig 12).

In the next experiment we consider the solution of the rotating cone problem, a variable coefficient linear advection problem. The initial condition, shown in Fig 13, is a cone of maximum height 1 and radius 0.15, centered at $x = 0.75, y = 0.5$. We set $a_x = 0.5 - y, a_y = x - 0.5$. The exact solution is counterclockwise rotation of the initial data about $x = 0.5, y = 0.5$. The numerical solution at $t = 1.0$ obtained by the modified scheme is shown in Fig 14. The $\max(V_n) = 0.66 < 1.0$ and $\min(V_n) = 0.0$ at $t = 1.0$.

The last experiment is the Buckley-Leverett equation describing two phase flow through porous media(e.g, water displacing oil):

$$u_t + \nabla \cdot [\vec{a}(x)f(u)] = 0,$$

where u refers to the saturation of one of the fluids(water), $\vec{a}(x)$ represent the two dimensional velocity field (i.e. $\vec{a} = (\frac{\partial \phi}{\partial x}, \frac{\partial \phi}{\partial y})^T$ and the potential $\phi = \frac{1}{100} \log(\sqrt{x^2 + y^2})$) in this experiment, $f(u)$ is typically a nonconvex function derived from laboratory measurements. Here we take

$$f = \frac{u^2}{0.2 - 0.4u + 1.2u^2}.$$

We solve Buckley-Leverett equation with initial data $u_o = 0$. Water is continuously injected in the lower left hand corner ($u_i = 1$); symmetry boundary conditions are imposed on left and lower boundaries. The solution contour at $t = 15$ is shown in Fig 15. The numerical solution satisfies the maximum principle (at $t = 15$, $\max(V_n) = 1.0$ and $\min(V_n) = 0.0$).

Acknowledgement I am grateful to my advisor Professor Stanley Osher for his careful reading of my manuscripts, his helpful advice, support, and forbearance.

References

- [1] Louis J. Durlofsky, Bjorn Engquist and Stanley Osher, "Triangle Based Adaptive Stencils for the Solution of Hyperbolic Conservation Laws", *J. Comput. Phys.*, to appear.
- [2] Chi-Wang Shu, Stanley Osher, "Efficient Implementation of Essentially Non-oscillatory Shock-Capturing Schemes, II", *J. Comput. Phys.*, Vol. 83, No. 1, July 1989.

- [3] Bernardo Cockburn, Suchung Hou, and Chi-Wang Shu “ The Runge-Kutta Local Projection Discontinuous Galerkin Finite Element Method For Conservation Laws IV: The Multidimensional Case ”. *Math. Comp.*, Volume 54, Number 190, April 1990, Pages 545-581

Fig 6

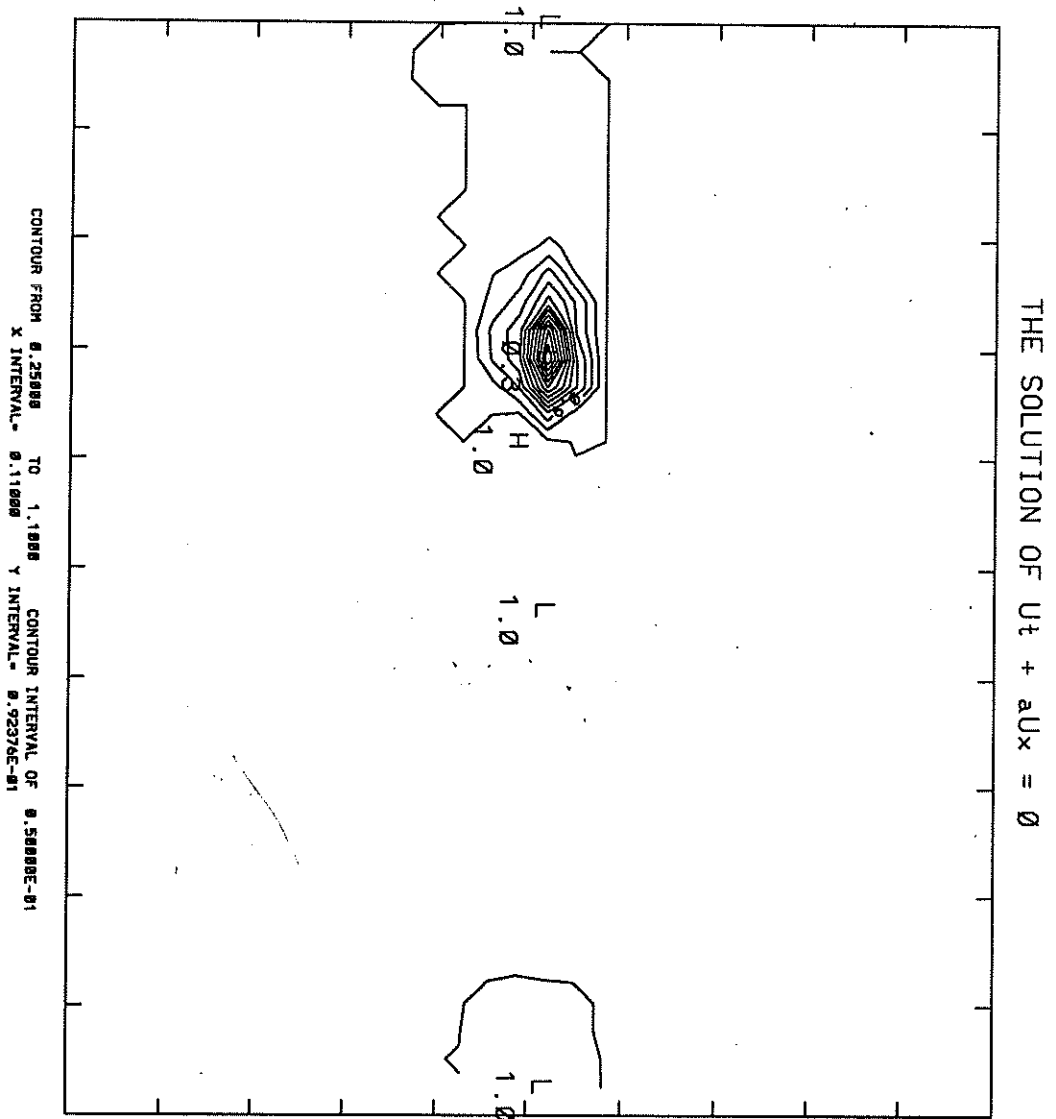


Fig 7.

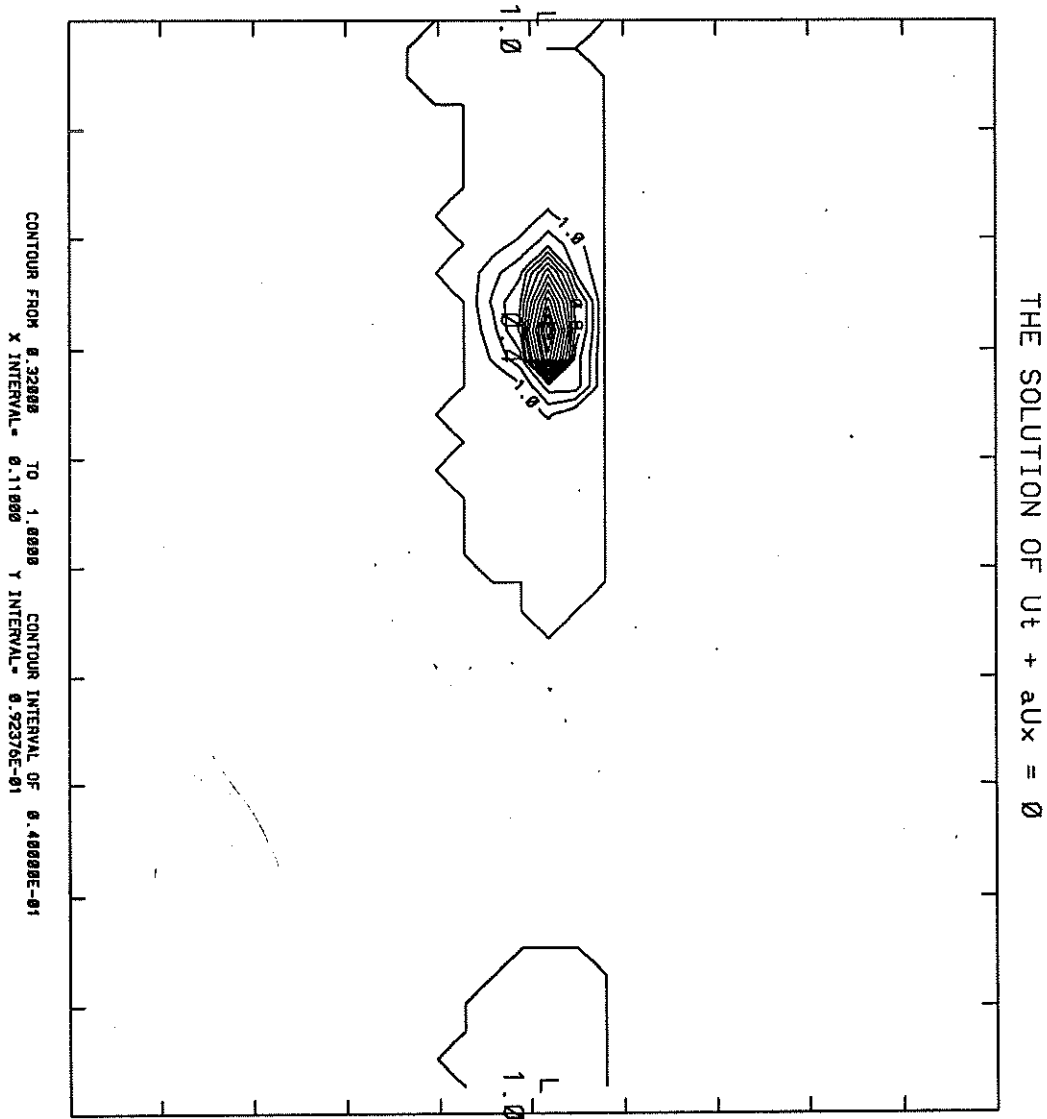


Fig 8

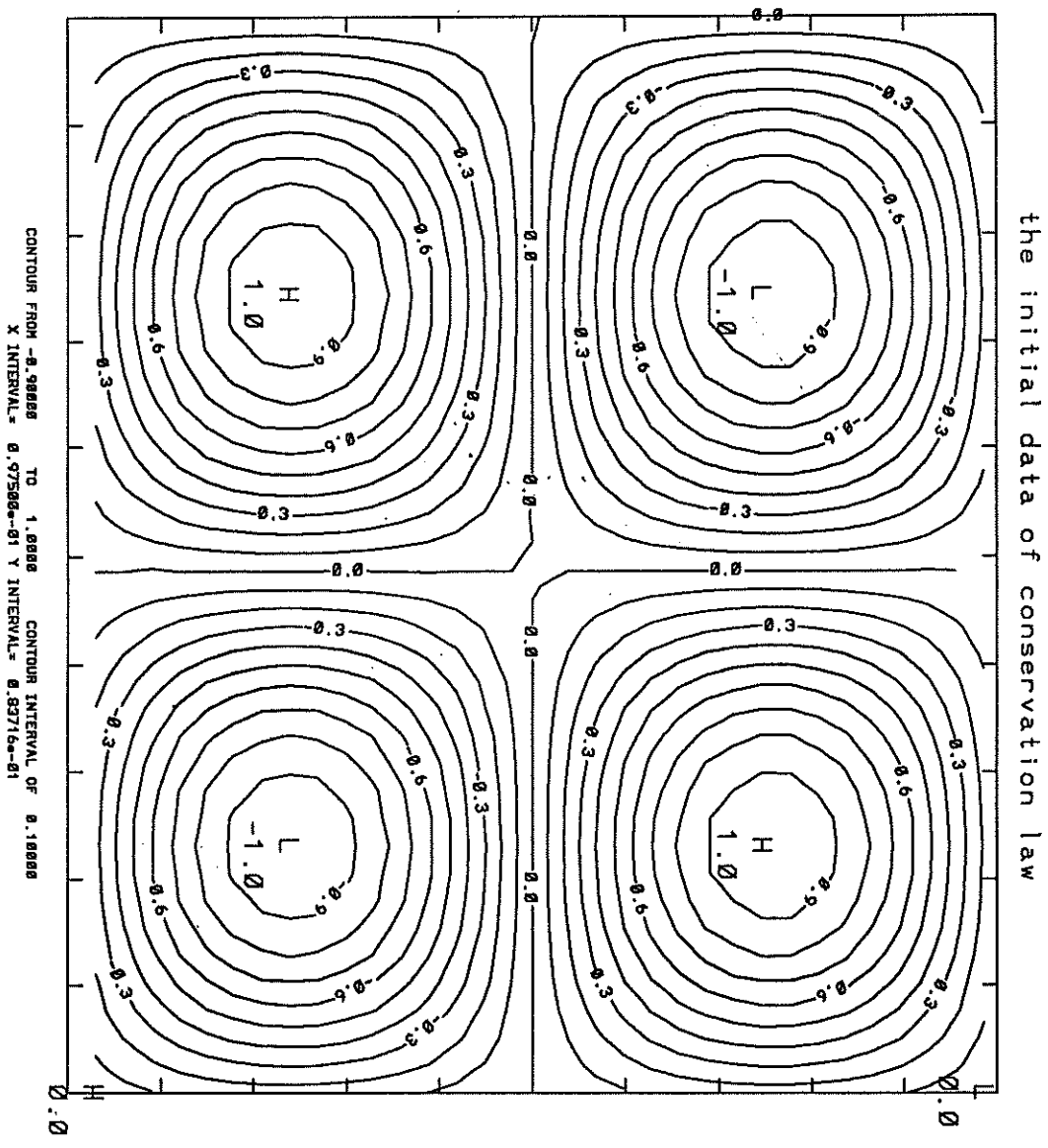


Fig 9

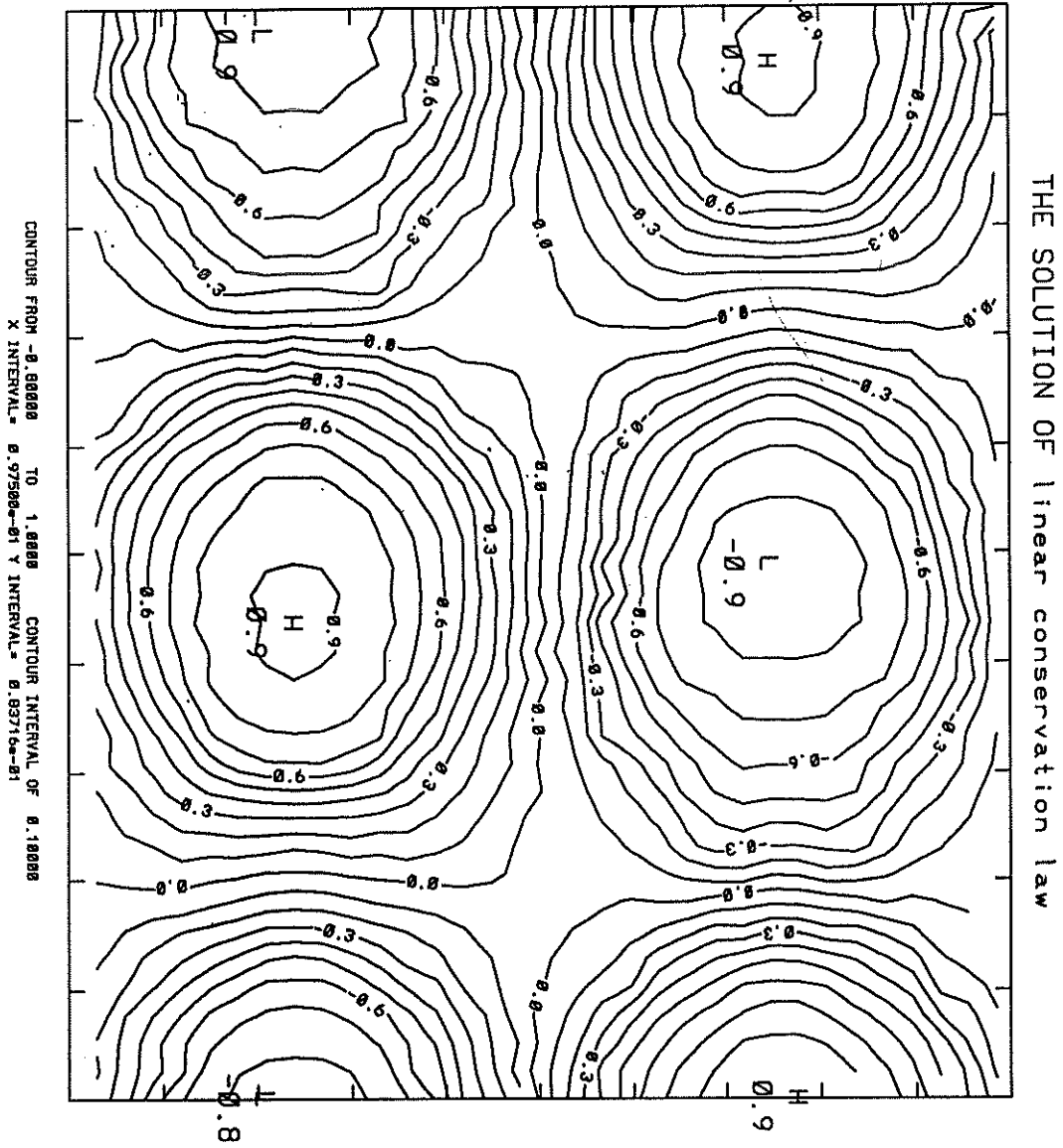


Fig 10

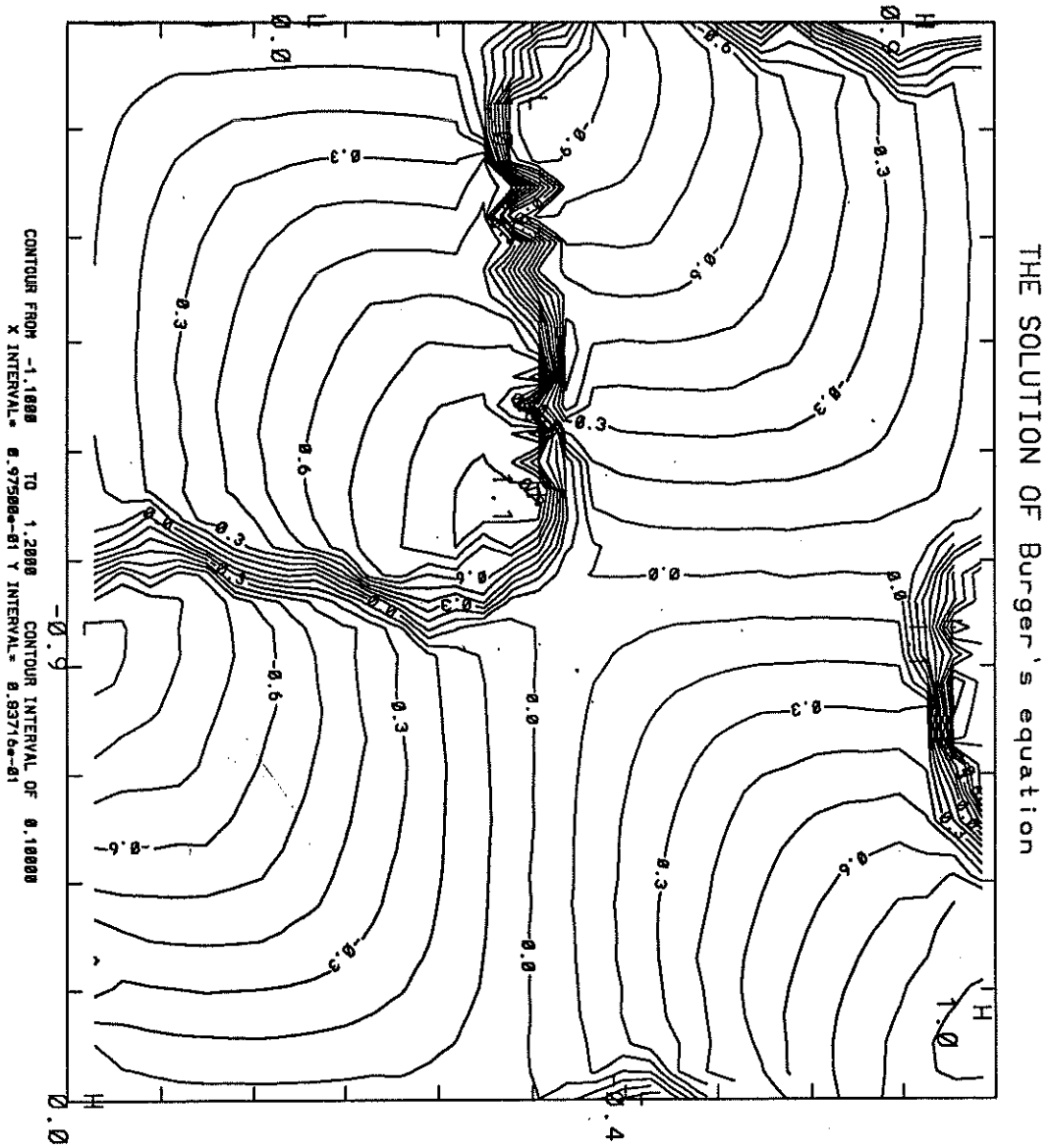


Fig 11

THE SOLUTION OF Burger's equation

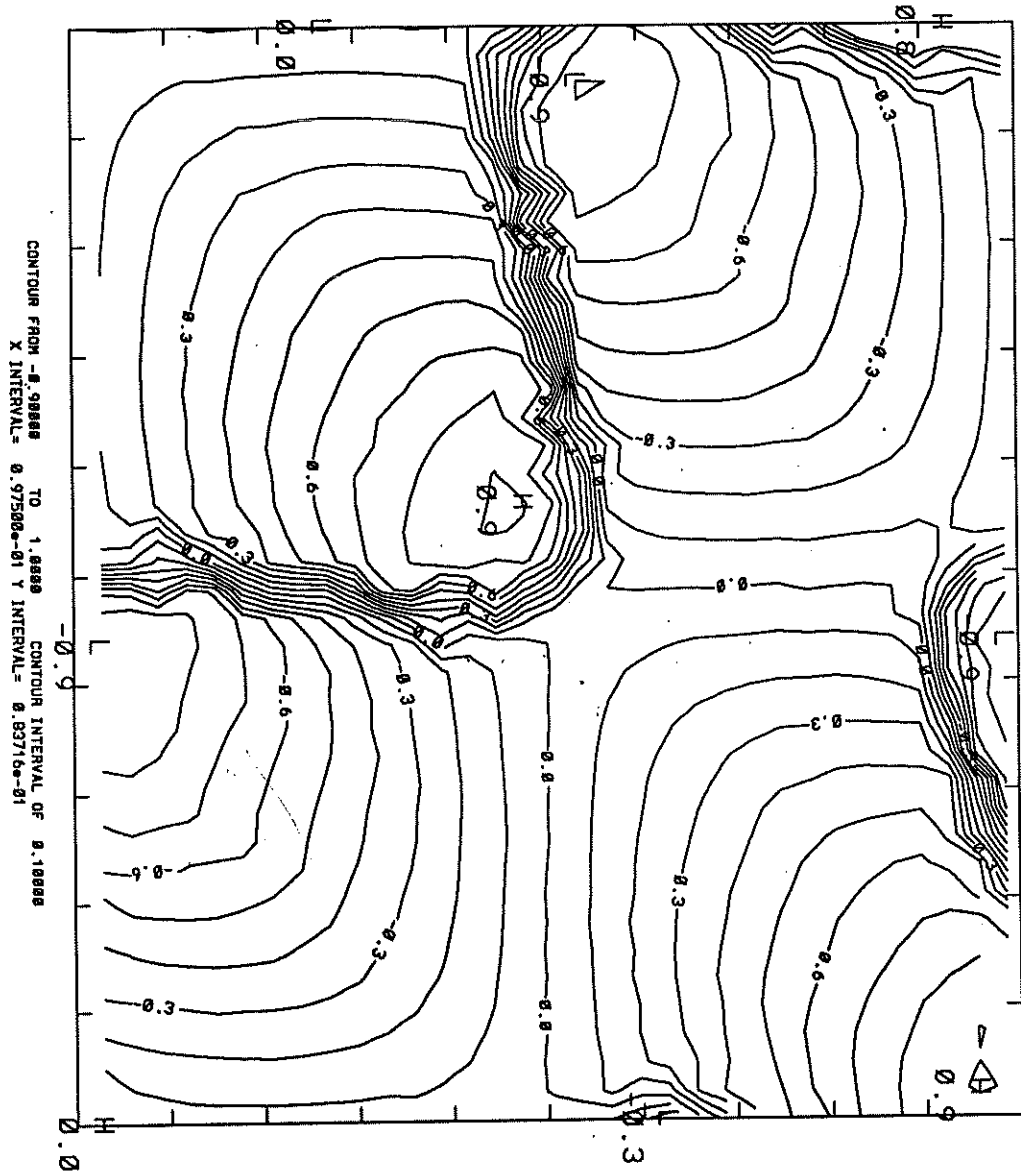


Fig 12

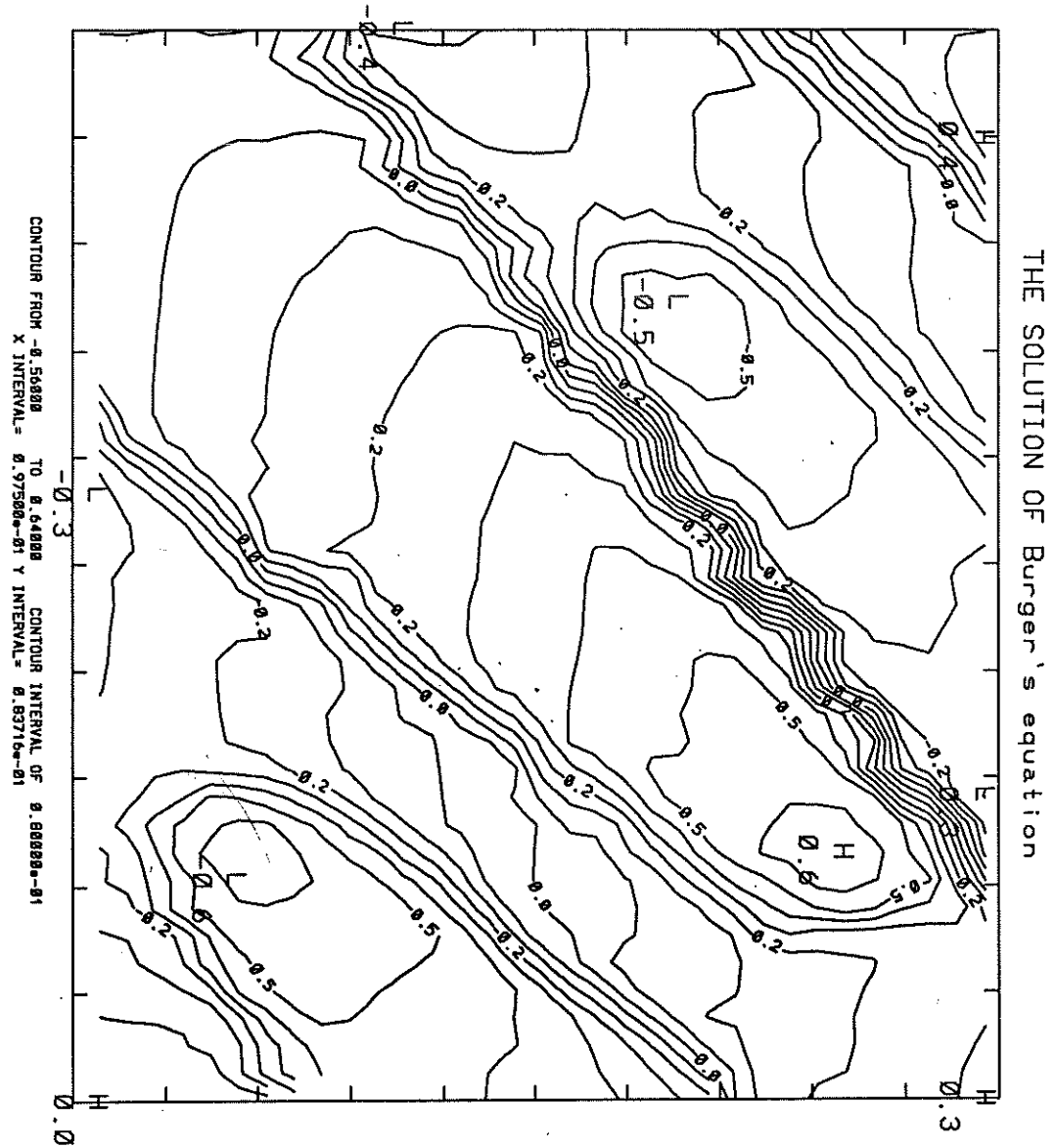


Fig 13

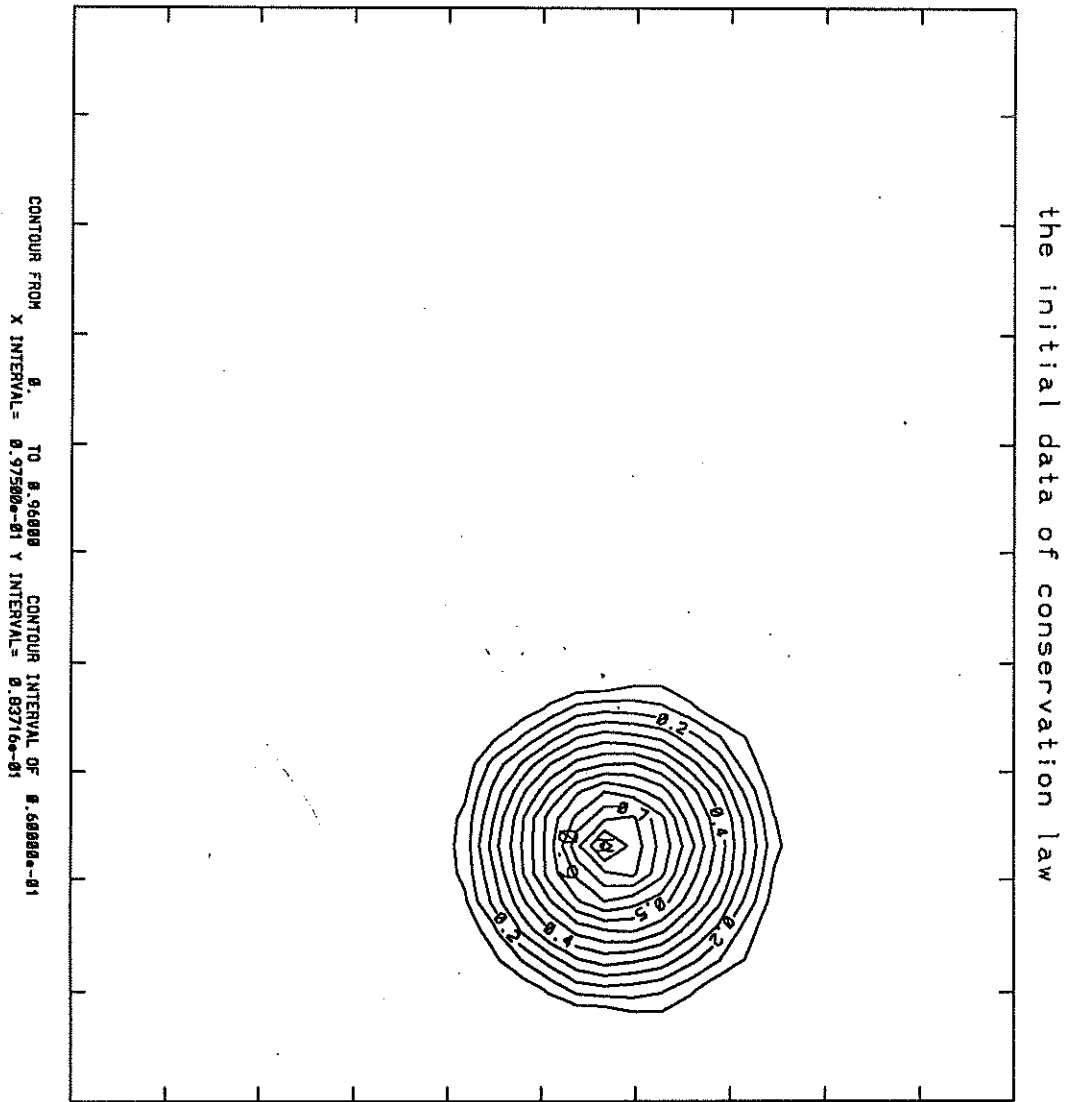


Fig 14

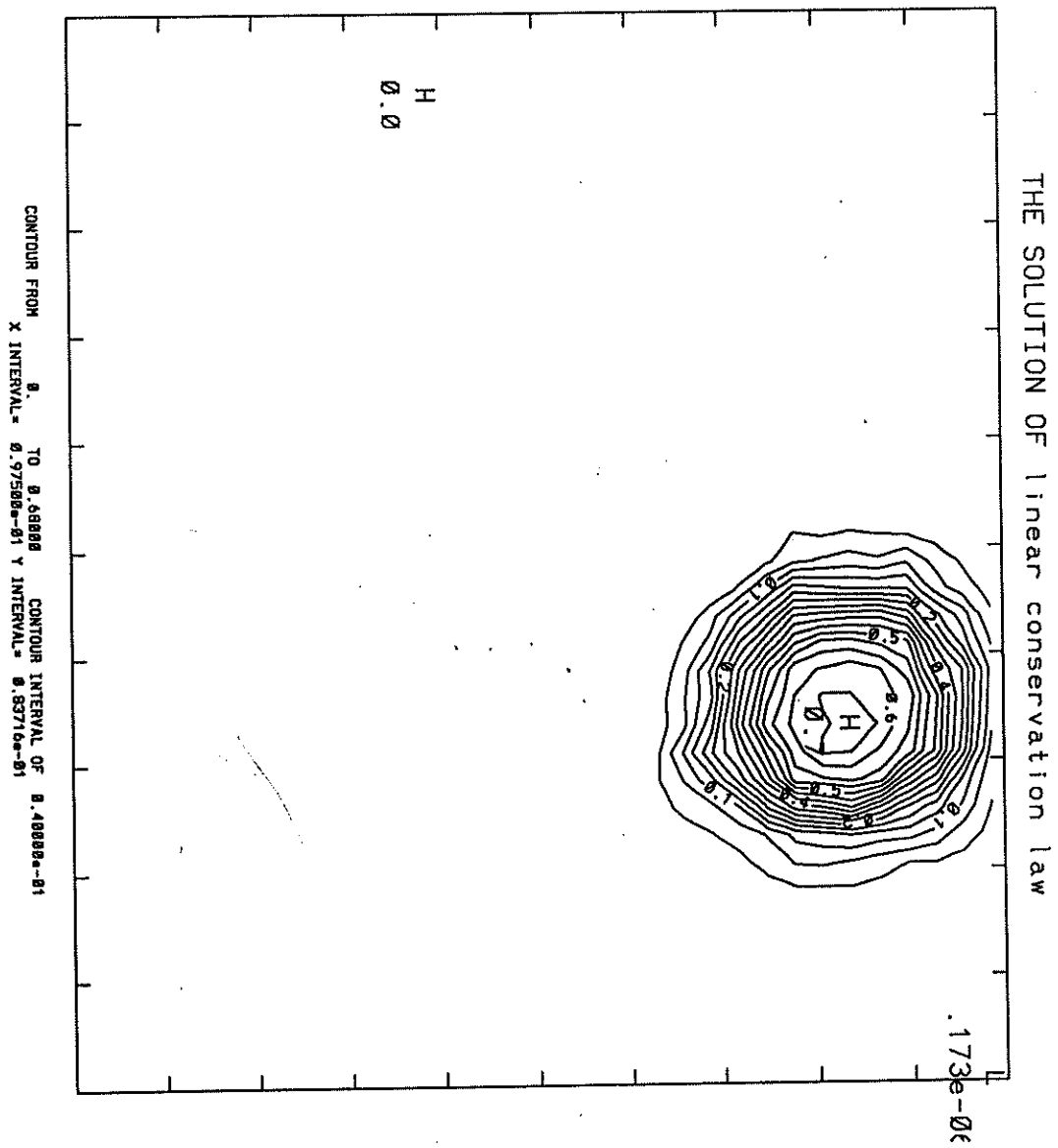


Fig 15

